Hindawi
Nanomaterials and Nanotechnology
Volume 2024, Article ID 9912599, 14 pages
https://doi.org/10.1155/2024/9912599

Research Article

Grewia tenax-Mediated Silver Nanoparticles as Efficient Antibacterial and Antifungal Agents

Priyanka Yadav,[1] **Monisha Singhal**,[1,2] **Sreemoyee Chatterjee**,[1] **Surendra Nimesh**,[3] **and Nidhi Gupta**[1]

[1]*Department of Microbiology and Biotechnology, IIS (Deemed to be University), Jaipur 302020, Rajasthan, India*
[2]*ICAR-National Research Centre on Meat, Hyderabad 500092, India*
[3]*Department of Biotechnology, Central University of Rajasthan, NH-8, Bandar Sindri, Ajmer 305817, Rajasthan, India*

Correspondence should be addressed to Nidhi Gupta; nidhi.gupta@iisuniv.ac.in

Received 26 June 2023; Accepted 25 November 2023; Published 5 January 2024

Academic Editor: Nico Lovergine

Nanoparticles have gained immense interest as probable drug molecules against microbial infections. Metal nanoparticles synthesized *via* exploring the reduction potential and capping activity of plants were found to have remarkable antimicrobial activity. The synthesis was conducted without hazardous chemicals and generation of toxic waste products. The focus of the study was, therefore, to investigate the efficacy of silver nanoparticles biosynthesized using *Grewia tenax* leaf extract as an antibacterial, antibiofilm, and antifungal therapeutic agent. The silver nanoparticles (GTAgNPs) were synthesized using optimized conditions of 2.5 mM $AgNO_3$ and 1 : 10 ratio of 10% extract at 37°C on continuous stirring. The characterization was done by UV-visible spectroscopy, DLS, SEM, zeta potential, and FTIR. The antibacterial activity of GTAgNPs against both Gram (+) *Bacillus cereus* and *Staphylococcus aureus* and Gram (−) *Escherichia coli* and *Pseudomonas aeruginosa* bacteria *via* zone of inhibition, MIC, and MBC was analysed. The inhibitory effect of silver nanoparticles on biofilm formation was also observed against these bacteria. These nanoparticles were then evaluated for their potential antifungal activity against *Candida albicans* and *Aspergillus niger* by observing fungal growth inhibition. The probable mechanism of antimicrobial activity by GTAgNPs was studied by scanning electron microscopy which showed the significant formation of pores on the cell surface in GTAgNPs-treated microbial cells, leading to the death of the microbial cell. All these studies concluded that GTAgNPs possess the potent antimicrobial potential and can be employed as antimicrobial therapeutic agents.

1. Introduction

Effective treatment strategies have been developed for eradicating common microbial infections. Despite the concerning approaches, the ever-increasing incidences of microbial infections commonly caused by parasites, fungi, viruses, and bacteria are alarming. Several common bacterial infections are caused by bacteria such as *Escherichia coli*, *Streptococcus pneumonia, Klebsiella pneumonia*, and *Staphylococcus aureus* [1]. Bacterial infections further cause several chronic infections and are the reason for the high number of mortalities, globally [2]. Therefore, the discovery of antibiotics is directed as a remarkable achievement in the medical field, from surgery to organ transplant and for various microbial infections and diseases. But bacteria have developed immunity against antibiotics which led to the occurrence of multidrug-resistant bacteria [3]. For decades, antimicrobial resistance (AMR) has been growing as a threat to the treatment efficacy of antiparasitic, antifungal, antiviral, and antibacterial drugs. Hence, antibiotic resistance, especially antibacterial resistance (ABR), has turned out as a dilemma in the medical field and public health, for treating patients.

To overcome this issue of antibiotic resistance, researchers are exploiting nanotechnology to develop nanoparticles as "nano-antibiotics" for targeted drug delivery without any drug resistance problem [4]. Nanoparticles (NPs) with a size

range of 1–100 nm can penetrate the bacterial cell wall, thus, in turn, impeding the bacterial biochemical pathways by destroying the cell organelles followed by bacterial cell death [1]. NPs generate reactive oxygen species (ROS) which damage the bacterial cell membrane [5], as well as target several cellular pathways simultaneously, making it impossible for the bacteria to develop resistance against them [6]. Due to the direct interaction and binding with the bacterial cell wall, there is no requirement for cell penetration and NPs can be used as alternatives to antibiotics, and their mode of action is irrelevant to the majority of the antibiotic resistance mechanisms [2].

Unique properties of nanoparticles, such as size, large surface area, exceptional mechanical strength, high stability, and lower melting points, make NPs the best candidate as drug carriers for several clinical applications [7]. These properties drove the interest of researchers from conventional synthesis to a biological synthesis approach, i.e., using biological systems for synthesis of nanoparticles, the process being termed as "green synthesis" [1].

The green synthesis of metallic NPs (Ag, Zn, Au, etc.) is gaining global acceptance by the scientific community [1, 8] due to its cost-effectiveness, ease of synthesis, biodegradability, nontoxicity, and environmental benignity [9–11]. Several types of NPs have attracted interest for their properties in the field of biomedical applications. Carbon-based NPs gained interest because of their interesting biomedical applications owing to the biocompatibility. Carbon NPs are extensively studied in several forms, from bulk to nanoscale [12], along with their methods of preparation and modelling [13]. Moreover, among a variety of nanomaterials, currently available in biomedical and biosensing research, silicon nanoparticles [14] are biocompatible and biodegradable and exhibit peculiar physicochemical properties, making Si-based nanostructures one of the most promising candidates as theragnostic material. Furthermore, among the metallic NPs, it is necessary to mention gold NPs (AuNPs) prepared by different methods [15] that attract the interest of researchers due to their enormous diagnostic importance of several diseases including diagnosis of cancer or imaging capabilities related to their optical properties, such as exhibiting a strong surface plasmon resonance [16].

Silver nanoparticles (AgNPs) have gained much popularity and are known to be a material of the future [17]. Recently, nanotechnologists in the field of biomedical science are more concerned with the biogenic/green synthesis of AgNPs to conquer the major drawbacks associated with conventional approaches. Plants have gained attention as a production assembly for the green synthesis of silver nanoparticles, whether from their fruit, seed, leaf, stem, bark, flower, or root extracts [18, 19]. Plant-mediated synthesis provides an eco-friendly, cost-effective, rapid, operative, and nontoxic/non-pathogenic approach with only a single-step technique for the biosynthesis of silver nanoparticles [20, 21]. Biomolecules or biocomponents of the plant(s) (phytochemicals) serve as reducing and stabilizing agents for silver ions.

Hence, to solve the problems associated with the non-biological synthesis approach of AgNPs and to explore a new mode of antimicrobial therapeutic agent, this study has been designed. The research work aims to develop a biological/green approach to synthesize silver nanoparticles using *Grewia tenax* plant leaf extract and testing these GTAgNPs for their antimicrobial activity with a special focus on antibacterial activity against Gram-positive (*Bacillus subtilis* and *Staphylococcus aureus*) and Gram-negative (*Escherichia coli* and *Pseudomonas aeruginosa*) bacterial strains and antifungal activity against *Aspergillus niger* and *Candida albicans*. This work gives us more insights into the applications and mechanism of biological therapeutics of green synthesized silver nanoparticles from *Grewia tenax*, a plant known for its medical ailment properties. This study might prove useful in future selection of biogenic AgNPs for their antimicrobial applications to use as alternatives to antibiotics for the benefit of patients as well as the environment.

2. Materials and Methods

2.1. Materials. Fresh and disease-free leaves of *Grewia tenax* were collected from neighbourhood nurseries in Mansarovar, Jaipur, India, and identified from the University of Rajasthan, Jaipur, India. All the chemicals were of analytical grade and obtained from HiMedia Laboratories Pvt. Ltd., India, and Sigma Aldrich, St Louis, Missouri, USA. The bacterial and fungal cultures were obtained from the Central Government-approved MTCC facility of IMTECH, Chandigarh, India.

2.2. Preparation of Grewia tenax Leaf Extract. Fresh leaves of the plant were thoroughly washed and dried for two to three days under shade before they were ground to powder form. The powdered leaves were used to prepare 10% (w/v) extract by heating at 60°C for 20 min with continuous stirring. Then, the mixture was cooled and filtered through Whatman filter paper No. 1 with reduced pressure conditions. This extract was utilized for NP synthesis and stored at −20°C for future use.

2.2.1. Biosynthesis and Optimization of Parameters for Silver Nanoparticles. Optimization of physical conditions was done following the rule of one variable at a time (OVAT). The extract used was prepared by dissolving 10 g of leaves powder in 100 ml water. Under the process, for the green synthesis of GTAgNPs, different volumes of extracts (50 μl of extract in 950 μl of $AgNO_3$ solution; 100 μl of extract in 900 μl of $AgNO_3$ solution; 150 μl of extract in 850 μl of $AgNO_3$ solution; and 200 μl of extract in 800 μl of $AgNO_3$ solution so that the ratio used was 1 : 5, 1 : 7.5, 1 : 10, and 1 : 20) were added in a dropwise manner to the varying concentrations of $AgNO_3$ (1.0 mM, 1.5 mM, 2.0 mM, and 2.5 mM) solution under constant stirring at 600 rpm for varied time intervals and temperatures. Color variation was an essential indication for the synthesis of NPs. The synthesized nanoparticles were centrifuged and the pellet was washed three times with deionized water. Then, it was resuspended in deionized water, and formation of GTAgNPs was confirmed by UV-visible spectroscopy.

2.2.2. Optimization of Process Parameters. The essential parameters which are important in the process of biosynthesis of GTAgNPs including the time of reaction,

temperature, the concentration of $AgNO_3$, and the ratio of extract to $AgNO_3$ were addressed during the green synthesis of NPs. By varying one parameter and keeping other factors constant, the biosynthesis process was carried out for 10 minutes and UV-visible spectrum was recorded to determine the synthesis. After optimizing the time required for synthesis, other three factors such as concentrations of $AgNO_3$ (1.0, 1.5, 2, and 2.5 mM), temperature (4°C, 25°C, 40°C, and 60°C), and variable extract to $AgNO_3$ ratio (1 : 20, 1 : 10, 1 : 6, and 1 : 5) were analysed similarly and each time UV-visible spectrophotometric analysis was performed to conclude the best obtained yield.

2.2.3. Design Expert Systematic Optimization of GTAgNPs by Using Box–Behnken Design (BBD). Using Design Expert, Box–Behnken design (BBD) ver. 12.0 software (Stat-Ease Inc., Minneapolis, USA), the most significant parameters, i.e., volume of leaf extract, concentrations of $AgNO_3$, and reaction temperature, were chosen as self-regulating factors for optimization. The trial runs were performed, and based on experimental trials, polydispersity index (PDI) and size of particles were calculated by the dynamic light scattering (DLS) technique. BBD results were reviewed through mathematical modelling, and numerical desirability function along with graphical optimization essential for the biosynthesis of GTAgNPs was obtained. Various important parameters that were taken into consideration for BBD study are summarized in Table 1.

2.2.4. Physicochemical Characterization of GTAgNPs. The dispersed AgNPs were analysed using UV-visible spectrometry within 300–700 nm wavelength range. The method is useful to estimate the size, concentration, and aggregation level of the particles. Determination of the hydrodynamic diameter and polydispersity index of GTAgNPs was done using dynamic light scattering (DLS). The Brownian motion of the NPs causes the scattering of the projected laser light at varying intensities. The particles were dissolved in deionized water and sonicated for 15 min, before being screened with a 5 MW He-Ne laser run at 633 nm wavelength followed by scattered light at 173° angle.

To identify the functional groups responsible for the reduction and stabilization of GTAgNPs, Fourier transform infrared (FTIR) spectroscopy of both plant extract and NPs was carried out. For this, KBr was utilized for tablet construction and scanned in an array of 4000 to 450 cm^{-1}. The spectrum revealed possible interaction between Ag and the bioactive molecules present in the extract.

The microstructural study for evaluation of definite shape-size and surface morphology of GTAgNPs was performed by scanning electron microscopy (SEM), and the chemical components of these particles were studied by using EDX. In SEM, during the interaction of the electrons and the sample, a wide variety of signals arise which reveal a lot of information about the surface morphology of the particles. During this process, NP solution was first converted into a dry powder and mounted on a sample holder which is followed by coating with a conductive metal, such as gold, using a sputter coater. A focused fine beam of electrons is used to scan the sample. The surface characteristics of the sample were obtained from the secondary electrons emitted from the sample surface.

Table 1: Independent variables are taken for optimization parameters via BBD.

S. no.	Independent variables	Units	Low value	High value
1	$AgNO_3$ concentration	μl	20	40
2	Extract volume	ml	2	4
3	Temperature	°C	25	60

2.2.5. Antimicrobial Potential of GTAgNPs. The biosynthesized GTAgNPs were explored for their antimicrobial potential against Gram (+) and Gram (−) bacteria as well as against fungal strains. These particles were also evaluated for their potency in inhibiting the formation of biofilm.

(1) Minimum Inhibitory Concentration (MIC) and Minimum Bactericidal Concentration (MBC) of GTAgNPs. 2, 3, 5-Triphenyl tetrazolium chloride (TTC) assay was carried out to evaluate the MIC of the synthesized GTAgNPs. TTC was used as a chromogenic marker which got reduced to TPF (1, 3, 5-triphenyl formazan) in the presence of bacteria. 100 μl of 24 h bacterial culture was poured into a 96-well plate with increasing concentrations of GTAgNPs from 0.05 mg/ml to 1 mg/ml. 10 μl of freshly prepared TTC was added to each well. The plate was incubated for 24 h at 37°C, and the absorbance was read at 480 nm. In the presence of live bacterial cells, TTC got reduced to red formazan, which is directly proportional to the percentage of viable cells.

MBC was evaluated using broth dilution of MIC tests where no observable growth was seen followed by plating the cultures on an agar plate and incubating for 24 h at 37°C. The concentration at which no growth of bacterial colonies was observed was taken as the MBC.

(2) Estimation of Antibacterial Efficacy of GTAgNPs by Disc Diffusion Method. The antibacterial activities of GTAgNPs were evaluated against Gram-positive (*Bacillus subtilis* and *Staphylococcus aureus*) and Gram-negative bacteria (*Escherichia coli* and *Pseudomonas aeruginosa*) by disc diffusion assay taking into consideration the zone of inhibition. Bacteria were grown as primary culture in Luria broth for 24 h at 37°C. The secondary inoculum was taken as 1% of the primary inoculum and incubated till an O.D. of 0.4 at 600 nm was achieved. Secondary cultures were streaked on agar plates with a density of 10^5 CFU ml^{-1}, and sterilized discs were placed on plates and loaded with varying concentrations of GTAgNPs (0.25, 0.5, 0.75, and 1.0 μg). The plates were then incubated overnight at 37°C, and the zone of inhibition was measured [22].

2.2.6. Antibiofilm Activity of GTAgNPs

(1) Congo Red Assay. The antibiofilm activity of GTAgNPs was studied against four strains of bacteria (*B. cereus*, *S. aureus*, *E. coli*, and *P. aeruginosa*) using BHI agar media

supplemented with sucrose (5%) and Congo red (0.08%). 24 h grown cultures of these four strains were streaked on Congo red agar plates with and without GTAgNPs and kept at 37°C for 24 h. The positive results in terms of formation of biofilm by microorganism were indicated by the occurrence of black colonies having a dry crystalline consistency.

(2) Microtiter Plate Assay (Crystal Violet Assay). The microtiter plate assay is performed for the quantitative evaluation of the antibiofilm efficiency of the biosynthesized GTAgNPs. It is an indirect method for the estimation of bacteria *in situ*. For 24 h, grown bacterial cultures (*B. cereus*, *S. aureus*, *E. coli*, *and P. aeruginosa*) were taken and adjusted to 0.5 McFarland's standard. The individual wells of the microtiter plate were filled with 180 μl of BHI broth and 10 μl of 24 h grown bacterial cultures. 10 μl of GTAgNPs, varying in concentration (0.25, 0.5, 0.75, and 1.0 μg), was added in each well (except control wells), and cultures were then incubated overnight at 37°C. After incubation, the plated cultures were washed thrice with 200 μl of phosphate buffer saline (PBS, pH-7.2) to remove any nonadherent bacteria. To fix the sessile organisms in wells, each well was treated with 200 μl of 2% sodium acetate. The wells were air-dried and then 200 μl of 0.1% (v/v) crystal violet (CV) dye was added to each well and then washed multiple times. The dye incorporated by the adherent cells was solubilized with 200 μl of 95% (*v*/ *v*) ethanol. The concentration of CV was determined by measuring the optical density of the solution at 595 nm using a microtiter plate reader.

2.2.7. Mechanism of GTAgNPs' Antibacterial Activity by SEM. To understand the mode of action of AgNPs against bacteria, SEM was done to observe the changes that occur on the cell surface for nanoparticles-treated and untreated bacterial culture. For the study, *B. subtilis* was grown in the presence and absence of GTAgNPs, and SEM was performed. Slides were prepared for the cultures, heat fixed, and stained with 2.5% glutaraldehyde followed by washing with PBS for three times. A dehydration series of ethanol (30%, 50%, 70%, 80%, 95%, and 100%) was done before air-drying [23]. These prepared slides were coated with gold and analysed under SEM.

2.2.8. Antifungal Assay

(1) MIC and MFC Determination of GTAgNPs Using Broth Dilution Method. The biosynthesized GTAgNPs were tested against *Aspergillus niger* and *Candida albicans* for their antifungal proficiency. The strains of both were maintained on PDA and YMA, respectively, at 28°C for 24 h. The MIC value was well defined based on visual inspection of fungal growth at different concentrations of nanoparticle suspensions. In this, two sets of tubes with 5 ml PDB were taken to which different concentrations of GTAgNPs (5, 7.5, 10, and 12 μg/ml) were added. PDB alone was taken as negative control, and amphotericin B at 20 μg/ml was taken as the positive control. These tubes were inoculated with 20 μl of diluted fungal spore suspension and incubated for 3-4 days at 28°C. Based on visualization, MIC values were taken which were further confirmed by taking O.D. at 600 nm.

(2) Disc Diffusion Assay. The antifungal efficiency of GTAgNPs was studied against *A. niger* and *C. albicans* by performing a disc diffusion assay. The colonies of *A. niger* and *C. albicans* were obtained on potato dextrose agar and yeast malt agar plates, respectively. Then, spore suspension broth was prepared in Tween 20 (0.02%), and standard (0.5) McFarland's solution was used for regulating turbidity. Prepared plates of PDA and YMA were used for harvested spores. Sterile discs impregnated with different concentrations of GTAgNPs (2.5, 5, 7.5, 10, and 12 μg/ml) were placed on seeded PDA and YMA plates along with negative (distilled water) and positive controls (amphotericin B 20 μg/ml). Incubation of plates was done at 28°C for 48 h and inhibition zones were measured.

(3) Colony Growth Assay. For colony growth inhibition assay, different concentrations of GTAgNPs (5, 7.5, 10, and 12 μg) were incorporated in PDA and YMA plates along with both negative (only PDA and YMA) and positive (PDA and YMA with amphotericin B 20 μg) controlled plates. Afterward, the cultures of *A. niger* and *C. albicans* were introduced at the centre of each PDA and YMA plate (6 mm wells) individually. Incubation was done for 3–5 days at 28°C to monitor the retardation of growth, and the growth inhibition rate was calculated using the formula mentioned below:

$$\text{Percentage growth inhibition} = \left[\frac{C - T}{C}\right] \times 100, \quad (1)$$

where C is the diameter of the negative control colony and T is the diameter of the treatment colony.

2.2.9. Mechanistic Study of GTAgNPs' Antifungal Activity. For studying the mechanism of action of GTAgNPs on *Aspergillus niger*, SEM was conducted. For this, 100 μl of treated and untreated liquid fungal cultures was centrifuged at 6,000 rpm for 10 minutes. The supernatant was discarded and the pellet was resuspended in sodium-phosphate buffer (100 mM, pH 7.0) by gentle inversion. A drop from this suspension was placed on the slide and air-dried. Dehydration series of ethanol (30%, 50%, 70%, 80%, 95%, and 100%) for the preparation of air-dried slides was carried out for 10 minutes in each step. Afterward, the gold coating was done on the slides to enhance the quality of the image.

3. Results and Discussion

The plant of *Grewia tenax* was submitted for identification to the Department of Botany, University of Rajasthan, Jaipur, India, and the reference number obtained was RUBL 21279. Leaves of the plant were then collected, dried, powdered, and sieved to obtain a fine powder that was used to prepare AgNPs using silver nitrate. These biosynthesized NPs were investigated for their antimicrobial activity against bacteria and fungi.

3.1. Biosynthesis of Silver Nanoparticles Using Grewia tenax Leaf Extract and Optimization of Reaction Parameters. Biological preparation of AgNPs involved using plant extracts which is a more environmentally sustainable approach. For this, an extracellular strategy was followed where we used 2.5 mM $AgNO_3$ and 10% extract prepared from the dried powder of leaves of *Grewia tenax* in a ratio of 1 : 10 in a dropwise manner. Several phytochemicals such as flavonoids, terpenoids, polyphenols, and alkaloids are present in the leaf extract of *Grewia tenax* that might play a dual role in the synthesis of AgNPs. These phytochemicals may act as reducing as well as stabilizing agents in the biogenic preparation of AgNPs. The reaction mixture was stirred continuously for 5 minutes at room temperature, and once the color change was visualized (Figure 1(a), top panel), it was read by UV-visible spectroscopy in the range of 300–700 nm.

The surface plasmon resonance (SPR) spectrum of AgNPs synthesized using plant extract showed a distinct peak at around 420 nm, confirming the presence of biogenic AgNPs as shown in Figure 1(b), lower panel. As explained by Brause et al., the obtained optical absorption spectrum of AgNPs is majorly dominated by SPR and the peak corresponded with particle size [24]. With the increase in the size of the particles, a shift to longer wavelengths can be observed in the SPR spectra of metallic nanoparticles. Also, it can be concluded that fabricated AgNPs were isotropic and spherical as a single SPR peak was observed.

3.2. Physicochemical Characterization of Nanoparticles

3.2.1. Box–Behnken Design- (BBD-) Based Evaluation of Experimental Conditions. To have monodispersed and optimum synthesis of NPs, physicochemical conditions such as concentration of $AgNO_3$, amount of extract, and the ratio of two along with temperature and time need to be standardized. For this, multivariate *in silico* tools are available to optimize the experimental conditions. We have employed one such tool, namely, Box–Behnken design (BBD), for 17 experiments which was established to zero down the best conditions for biogenic synthesis. The seventeen experimental trials established in BBD Design Expert version 12.0 that gave particle size and polydispersity index (PDI) are summarized in Table 2. These trial runs were then validated by wet experiments, and particles were analysed by dynamic light scattering (DLS) for the average size and zeta sizer for charge potential.

The data thus obtained in BBD were put under a quadratic polynomial model to generate diagnostic plots and evaluate them. As shown in Figures 2(a)–2(c), the model diagnostic plots obtained for response particle size gave a linear predicted vs. actual graph where it was observed that the predicted values were in close proximity with the actual ones. Perturbation plots were obtained to study the overall effect of all the selected factors, and the result showed that response is sensitive to factor B, i.e., extract volume to be used as a curvature in response to this factor is observed. The other two factors, factor A, i.e., $AgNO_3$ concentration, and factor C, temperature, also showed slight curvature. The interaction plots obtained were also showing bending patterns, indicating that all three factors play an important role in the biosynthesis of AgNPs and any fluctuations in the three factors would eventually affect the size (Figures 2(a)–2(c)) and PDI (Figures 2(d)–2(f)).

Three-dimensional (3D) response surface plots obtained are in agreement with two-dimensional (2D) contours. These plots evaluate the cumulative impact variations in all the variables on the size distribution of metallic nanoparticles. In our study, we observed that the predicted size range of the particles was 95–105 nm with changes in any of the three variables, indicating that there might be variations in the size of AgNPs with increasing concentrations of reactants and temperature (Figures 3(a)–3(f)). The actual size as analysed by DLS was found to be ~109 nm and the zeta potential was 0.321, very close to the one obtained by BBD, i.e., 105 nm at 25°C and PDI of 0.0547, as shown in Table 2.

3.2.2. Optimization with respect to Concentration of $AgNO_3$, Volume of Extract, and Temperature. Concentrations of $AgNO_3$, the percentage of extract, and the ratio of the two affect the size of synthesized particles. Also, temperature plays an important role in the synthesis of monodispersed, spherical AgNPs. We have, therefore, used varying concentrations of $AgNO_3$ and extract amounts to obtain the best suitable conditions for *Grewia tenax-mediated* synthesis of AgNPs. As summarized in Figures 4(a)–4(c), we identified that optimized conditions for GTAgNPs synthesis were 2.5 mM $AgNO_3$ and 1 : 10 v/v ratio for $AgNO_3$ to 10% extract, at 37°C in 10 minutes of continuous stirring. The temperature range from 25° to 60°C was found to be suitable for synthesis as a single, sharp peak was obtained when the SPR area was obtained by a UV-visible spectrophotometer. The narrow, sharp peak indicated the formation of monodispersed nanoparticles.

3.2.3. Size and Shape Analysis of Biosynthesized GTAgNPs. Size distribution of the formulated AgNPs along with the surface charge was analysed by DLS that revealed the hydrodynamic diameter to be around 109 nm with a zeta potential of 0.321 (Figures 5(a) and 5(b)), agreeing to have less polydispersity for the biosynthesized AgNPs.

To observe the morphology along with the size of GTAgNPs, scanning electron microscopy was conducted which showed that the particles formed were spherical with a smooth texture, and the average size was determined to be around 44 nm (Figure 6(a)). EDX analysis as summarized in Figure 6(b) showed that silver atoms were predominantly present with four Bragg's diffraction values. Yazdi et al. also reported the presence of four Bragg's diffraction values for silver nanoparticles biosynthesized using *Rheum turkestanicum* shoot's extract [25].

3.2.4. FTIR Analysis of Biogenic GTAgNPs. Fourier transform infrared (FTIR) spectroscopy tool helps understand the involvement of functional groups present in biomolecules

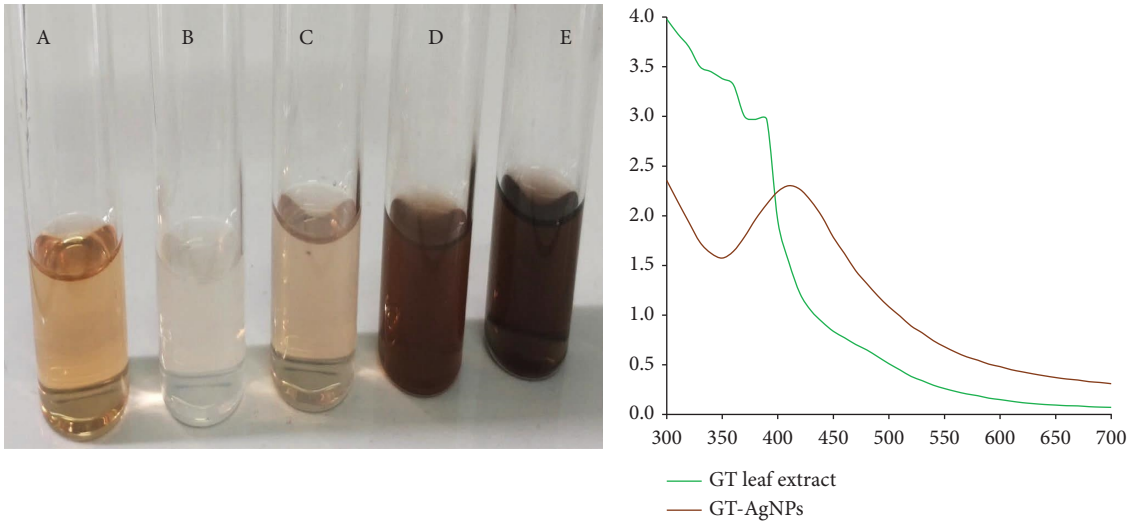

Figure 1: (a) Synthesis of GTAgNPs (C–E) shown by a transition in the color of silver nitrate solution (B) from colorless to deep brown color after the addition of extract (A). (b) UV-Vis spectra of GTAgNPs in the range of 300–700 nm, along with that of extract as reference.

Table 2: Experimental trial runs given by BBD.

S. no.	Run	$AgNO_3$ vol. (μl)	Extract vol. (ml)	Temperature (°C)	Particle size (nm)	PDI
1	2	20	2	42.5	92.3	0.14
2	4	40	2	42.5	97.2	0.274229
3	17	20	4	42.5	92.9	0.0375052
4	14	40	4	42.5	93.5191	0.966347
5	9	20	3	25	99.6493	0.845629
6	8	40	3	25	100.045	0.428665
7	5	20	3	60	103.548	0.459216
8	6	40	3	60	104.66	0.213908
9	11	30	2	25	97.1942	0.554521
10	12	30	4	25	105.701	0.0547038
11	1	30	2	60	94.9194	0.696856
12	13	30	4	60	107.563	0.247538
13	3	30	3	42.5	106.063	0.0603843
14	7	30	3	42.5	99.9837	0.799221
15	15	30	3	42.5	101.589	0.370139
16	16	30	3	42.5	104.54	0.239139
17	10	30	3	42.5	98.7665	0.928612

found in plant extract that helps in reducing $AgNO_3$ to AgNPs as well as in capping to provide stability to the synthesized AgNPs. The spectra were recorded both for the extract and the synthesized GTAgNPs following the range of 4000–400 cm^{-1} frequency. In the GT extract (Figure 7), the peak at 3427 cm^{-1} corresponding to OH stretching of polyphenols was observed which then moved to shorter frequency wavelengths in the obtained spectrum of AgNPs, clearly indicating the reducing role of hydroxyl groups of polyphenols present in the extract. The FTIR spectrum for GTAgNPs revealed major peaks at 2982–2980 cm^{-1} which stands for CH stretching, along with peaks at 1603 cm^{-1} (N-H stretching) and 1253 cm^{-1} (C-N stretching) [26]. The presence of relative peaks (Figure 7) confirmed the role of carboxylic acids and primary and secondary amine compounds in the capping of AgNPs.

3.3. Estimation of Antimicrobial Efficacy of Nanoparticles Using Various Methods

3.3.1. Antimicrobial Activity of Nanoparticles by Disc Diffusion Study. AgNPs are known for their biological applications such as antimicrobial activities. The literature recommends several studies that support the antibacterial activity of plant-based synthesized AgNPs. The green synthesis approach provides a better augmentation to the existing antimicrobial properties of the plant in terms of nanoparticles as the synergistic impact can be obtained in terms of the latter. NPs synthesized using plant extract help in reducing the concentration of the required doses for the activity against bacteria and fungi. In this study, we have chosen *Grewia tenax*, a locally grown berry that is used in rural and suburban regions of Rajasthan, India, for various

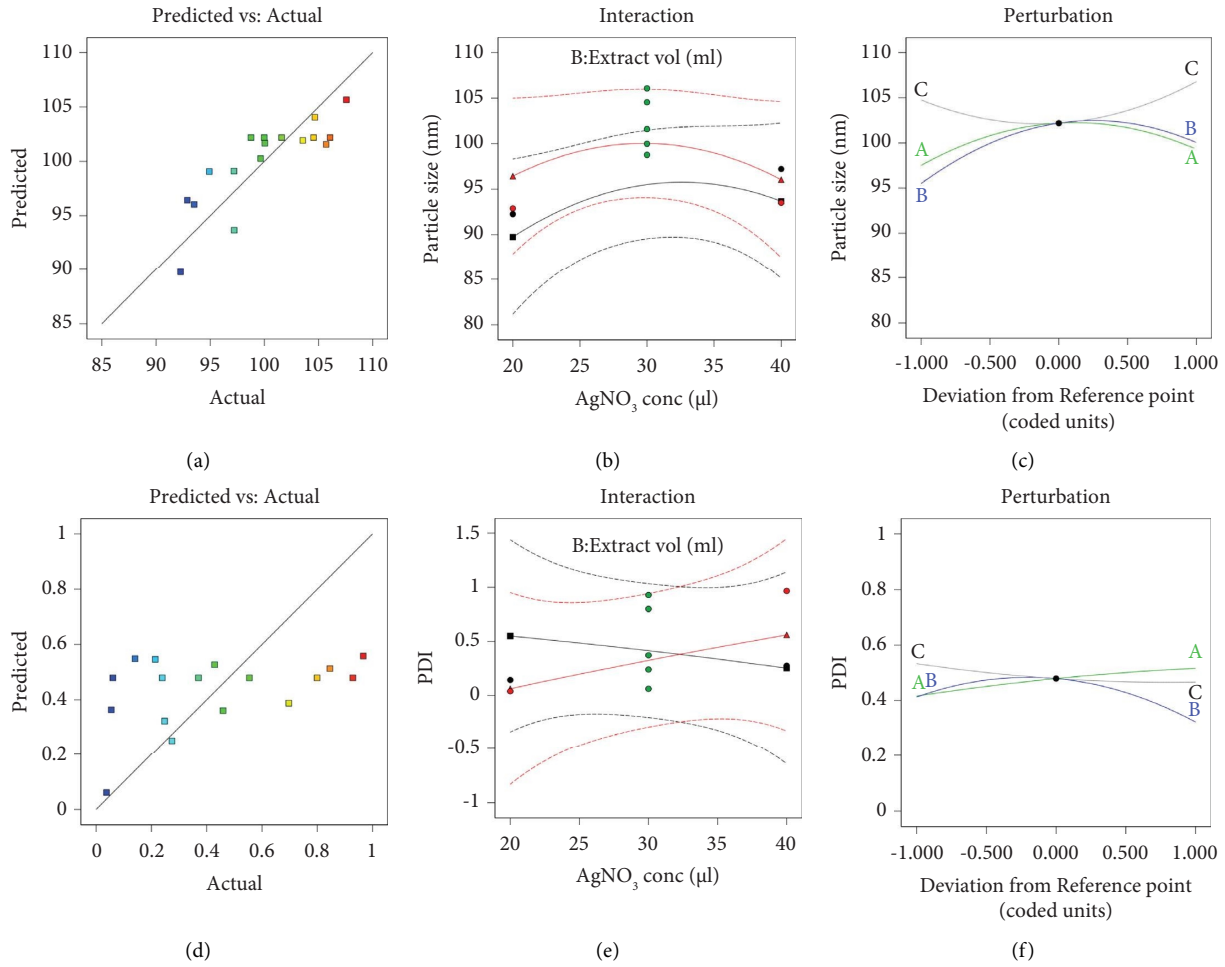

FIGURE 2: Model diagnostic plots of actual vs. predicted interaction and perturbation of response for silver nanoparticles in terms of size and PDI. (a) Representation of the actual particle size vs. the predicted particle size by BBD. (b) BBD evaluation of the effect on the particle size with variation in volume of the extract and $AgNO_3$ concentration. (c) Effect of temperature on the size of synthesized AgNPs as evaluated by BBD. (d) Evaluation of PDI linearity by BBD for actual vs. prediction. (e) Variation in volume of the extract vs. $AgNO_3$ concentration deviates PDI as observed. (f) BBD analysis showed deviation in PDI with variation in temperature.

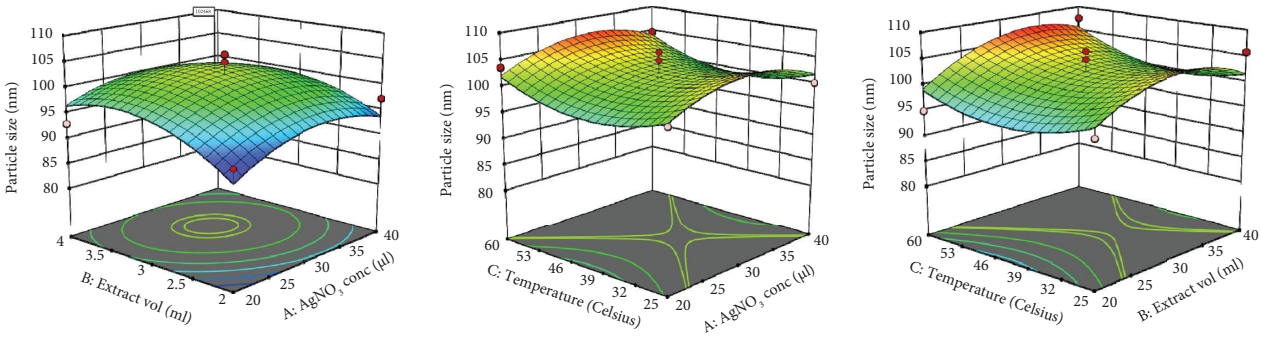

FIGURE 3: Continued.

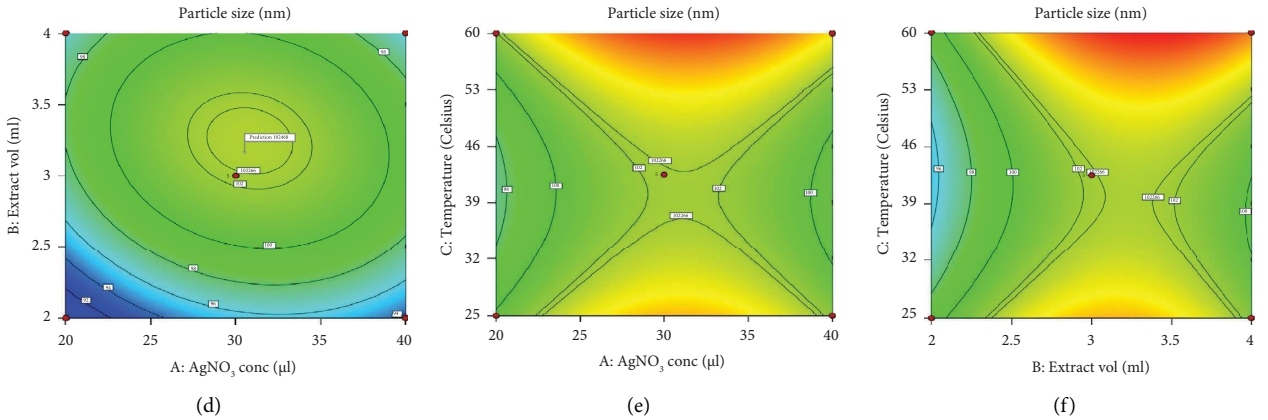

FIGURE 3: Three-dimensional (3D) response surface plots evaluate the cumulative impact variations for different variables ($AgNO_3$ concentration, extract volume, and temperature) on the size distribution of silver nanoparticles, which is in agreement with two-dimensional (2D) plots obtained by BBD for GTAgNPs. (a) and (d) are 3D and 2D plots for the effect on the size on AgNPs when variation in extract volume and $AgNO_3$ concentration is taken into consideration. Similarly, (b) and (e) represent 3D and 2D plots for deviation in the size of metallic nanoparticles if temperature and $AgNO_3$ concentrations are changed. Also, (c) and (f) gives BBD analysis of deviation in AgNPs size with different ranges of temperature and variable extract volume.

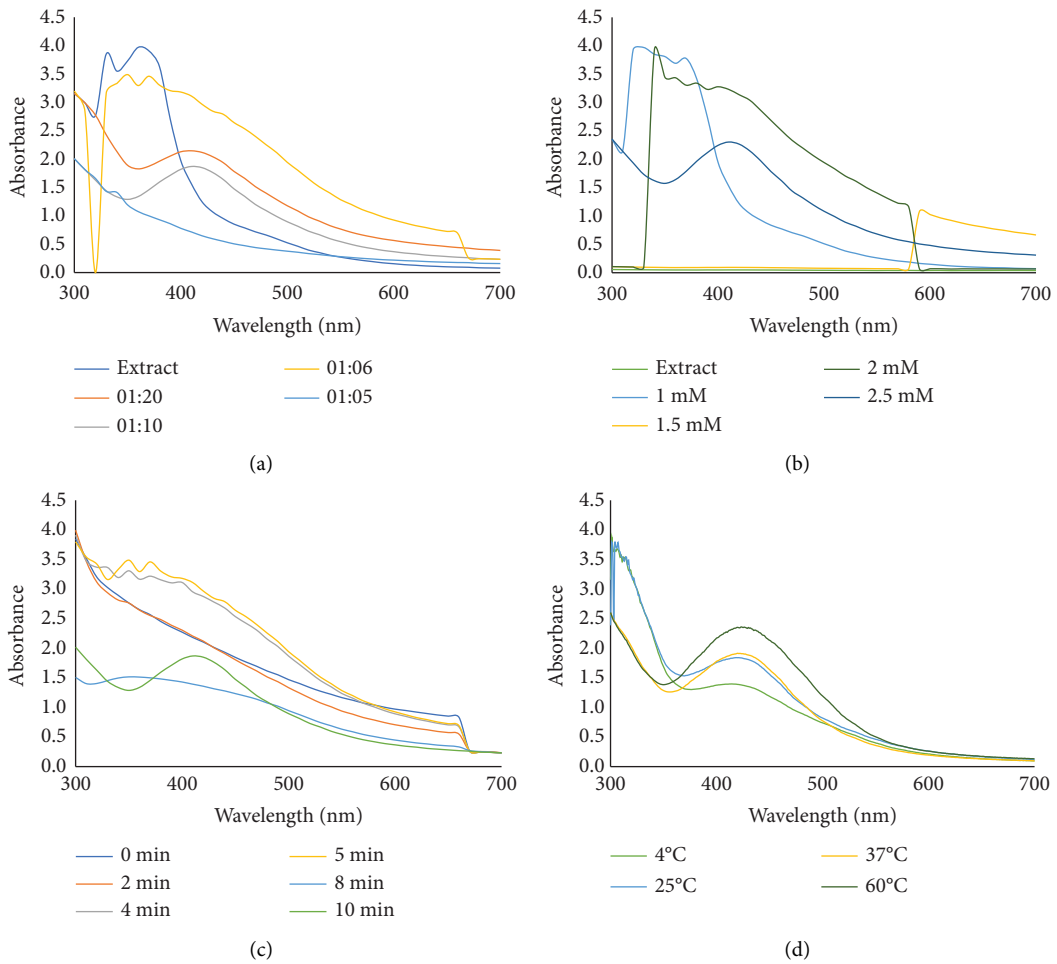

FIGURE 4: UV-Vis spectra for parameter optimization of GTAgNPs. (a) $AgNO_3$ and variable volume of extract ratio best obtained at 1 : 10. (b) Molarity of silver nitrate in the reaction mix found to be optimum at 2.5 mM. (c) Time duration of 10 minutes optimized for which reaction is allowed for stirring. (d) Temperature (37°C) at which reaction for biosynthesis is carried out.

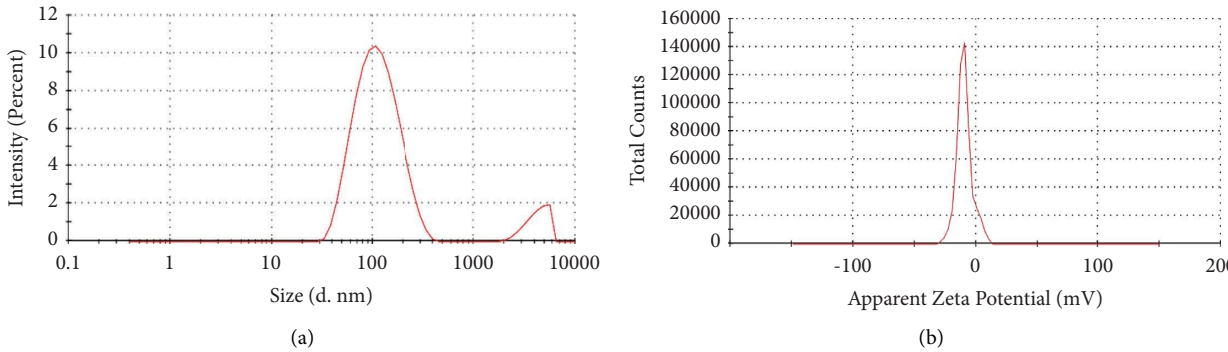

Figure 5: (a) The graphs depict the hydrodynamic diameter of GTAgNPs determined by dynamic light scattering which is ~109 nm with (b) zeta potential of synthesized GTAgNPs.

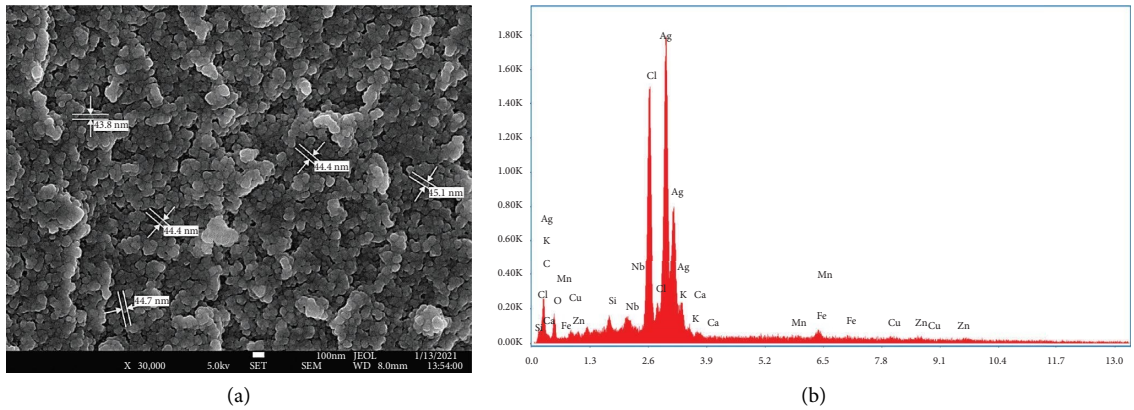

Figure 6: (a) SEM image of GTAgNPs showing smooth and spherical morphology with an average size of around 44 nm and (b) EDX analysis revealed the presence of silver in nanoparticle formation.

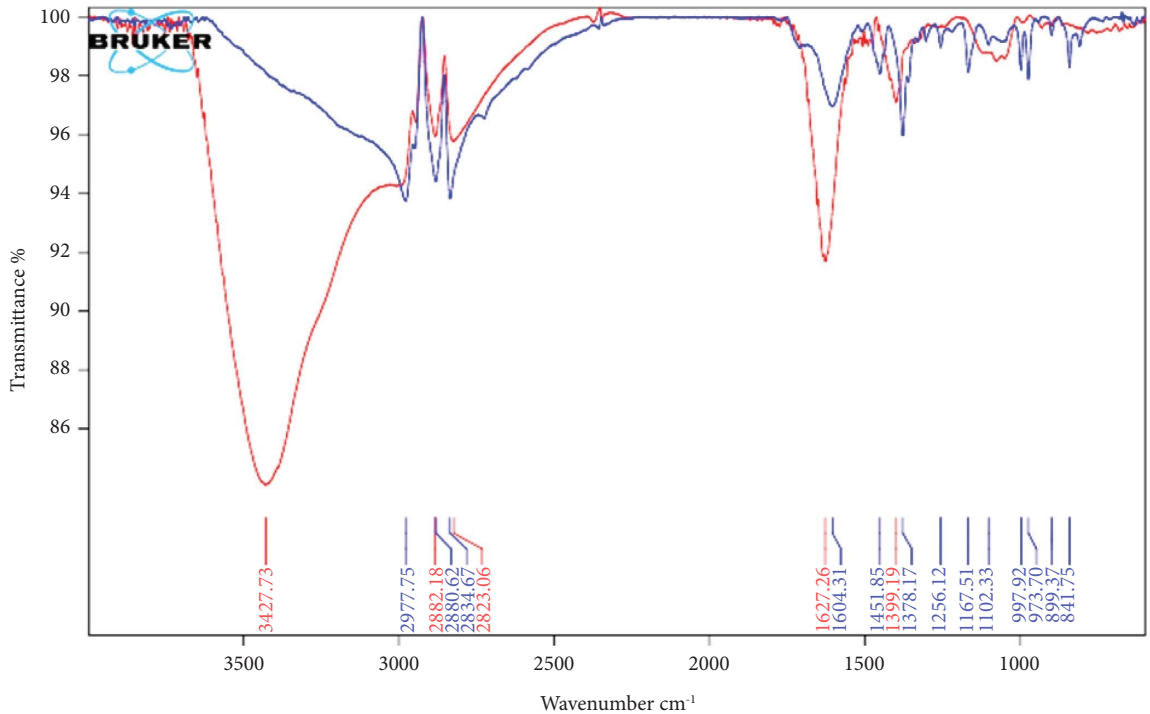

Figure 7: FTIR spectra of *Grewia tenax* leaf extract (in red) and biosynthesized GTAgNPs using the extract under optimized conditions (in blue).

Table 3: The zone of inhibition (mm) showing the antibacterial potential of GTAgNPs in a dose-dependent manner against Gram-positive and Gram-negative bacterial strains.

Bacterial strains	Positive control	Concentration (μg)			
		0.25	0.5	0.75	1
Pseudomonas aeruginosa	12 mm ± 1	4 mm ± 1	12.3 mm ± 1.52	17 mm ± 1	20 mm ± 1
Bacillus subtilis	6 mm ± 1	6 mm ± 1	12 mm ± 1	18 mm ± 1	22.7 mm ± 1.52
Escherichia coli	13 mm ± 1.63	6 mm ± 1	10 mm ± 1	14 mm ± 1	18 mm ± 1
Staphylococcus aureus	1.3 mm ± 0.577	4 mm ± 1	8 mm ± 1	12 mm ± 1	17 mm ± 1

stomach ailments. The antibacterial activity of the particles was assayed by observing the zone of inhibition, obtained by placing paper discs impregnated with AgNPs, water, and ampicillin as tests, negative control, and positive control, respectively. The zone of inhibition thus obtained for these is summarized in Table 3.

The activity of synthesized AgNPs was observed to be more potent in comparison to the positive control. In the case of Gram-positive bacteria, namely, *B. subtilis* and *S. aureus*, the antibacterial activity of AgNPs was 3–5 times more than the antibiotic ampicillin. The results demonstrated that GTAgNPs were able to penetrate the thick cell membrane of bacterial cells more potently to impart their antibacterial effect.

3.3.2. MIC and MBC Determination of Nanoparticles Using TTC Assay. Initially, the minimum inhibitory concentration (MIC) and minimum bactericidal concentration (MBC) of GTAgNPs were determined to calculate the minimal dose that is effective in reducing the growth of bacteria and responsible for the death of more than 99 percent of bacterial cells, respectively. The MIC was determined to be 0.5 μg for both Gram-negative and Gram-positive bacteria. MBC was observed to be 2.0 μg for Gram-negative bacteria, namely, *E. coli*, and 10 μg concentration was observed for *S. aureus*, i.e., Gram-positive bacteria. MBC is more for Gram-positive bacteria due to hindered accessibility of AgNPs through thick cell membranes.

3.3.3. Estimation of Antibiofilm Efficacy of Nanoparticles Using Congo Red and Crystal Violet Assays. Most bacteria impart their antibiotic resistance due to the formation of biofilm that is made of exopolysaccharides being secreted by the bacteria when present in a group. Biofilm has a defined structure and acts as a medium for genetic transfer and communication between cells [27]. Biofilm is an important health issue as medical devices harbouring biofilms are responsible for an array of microbial infections in patients and add burden on an already crippled healthcare environment [28].

Green synthesized AgNPs can be coated on medical devices and to an extent prevent postoperative infection as NPs are quite efficient in inhibiting the formation of biofilms as observed by our earlier as well as current studies [29–31]. In the present study, GTAgNPs were evaluated for their efficacy against biofilm formation in all four bacterial strains considered. Congo red agar assay (Figure 8(a)) clearly marked the inhibitory potential of AgNPs as shown by the absence of black colonies in the treated culture which are indications of secretion of exopolysaccharide for the formation of biofilms. Quantitative analysis by crystal violet assay also showed remarkable inhibition of biofilm formation in a dose-dependent manner as summarized in Table 4.

3.3.4. Evaluation of Antifungal Efficacy of GTAgNPs. Post COVID-19 pandemic, *Aspergillus niger* and *Candida albicans* have been observed to cause severe infections in case of health compromised patients, while no such symptoms have been observed in the case of healthy people [25, 26]. *C. albicans* is clinically important as it is responsible for catheter-related blood infections [32]. At times, antifungal treatment cannot be provided in time in such patients. AgNPs' efficacy can be studied in such scenarios as green synthesized nanoparticles can provide a solution to such comorbidities, but more detailed investigations are required. In our study, we evaluated the benefits of GTAgNPs against the two fungi. *In vitro*assays confirmed that even at a low concentration of 5 μg, AgNPs were able to significantly inhibit the growth of both the fungal strains as shown in Figure 9, by colony growth assays and broth dilution method. In comparison to amphotericin B, a known antifungal, GTAgNPs have exhibited almost 2-fold fungal growth inhibition. Fungi are more resistant to treatment due to their complex cell structure and advanced detoxification system [33], but our biosynthesized AgNPs have shown potent antifungal activity and this potential can be harnessed medically with further deep research investigations.

3.4. Analysis of the Mechanism of Antimicrobial Activity Exerted by GTAgNPs by SEM. The biosynthesized GTAgNPs were found to possess potent antibacterial and antifungal efficacy. As per a study conducted by Rama et al., biosynthesized AgNPs were observed to possess remarkable antioxidant potential along with antimicrobial efficacy [19]. The mechanism of the antimicrobial study was then studied by scanning electron microscopy (SEM) where AgNPs-treated and nontreated bacterial and fungal cultures were observed for change in cell surface morphology. On observation, it was revealed that untreated bacterial as well as fungal cells possess intact, smooth cell membranes, whereas pores were formed on the surface of nanoparticles-treated cells (Figures 10(a) and 10(b)). In certain instances, it was observed that the microbial cells were ruptured due to the binding of AgNPs on the cell surface.

Burdușel and coworkers explained that AgNPs work in a Trojan-horse fashion as their initial attachment to the cell surface causes permeability and respiration impairment,

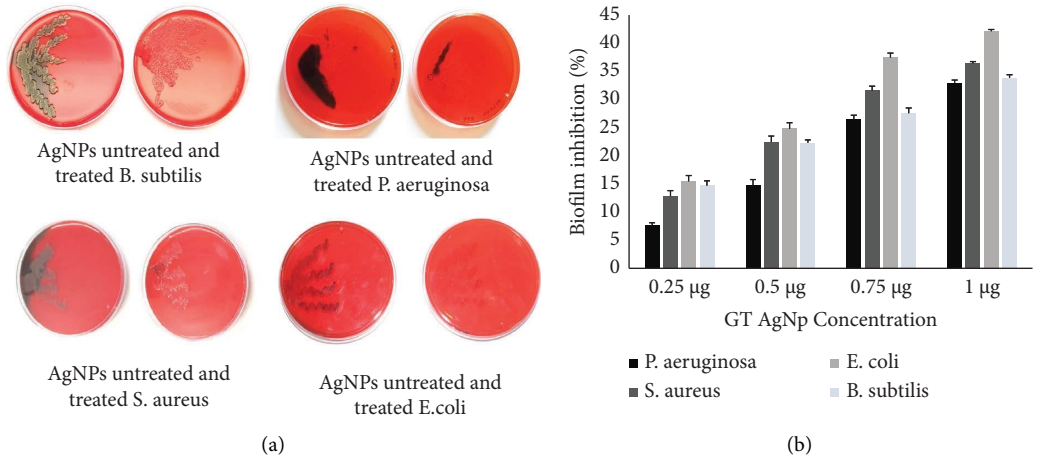

Figure 8: (a) Congo red agar assay showing antibiofilm efficacy of GTAgNP. The occurrence of black colonies marked biofilm production, whereas no such formations were seen in GTAgNP-treated bacterial strains. (b) Graphical representation of percentage biofilm inhibition in crystal violet assay.

Table 4: Quantitative estimation of biofilm inhibition (percentage) by crystal violet assay against Gram-positive and Gram-negative bacterial strains.

Bacterial strains	GTAgNP concentrations (μg)			
	0.25	0.5	0.75	1
P. aeruginosa	7.7 ± 0.477109	14.7 ± 1.030016	26.5 ± 0.725902	32.9 ± 0.484974
S. aureus	12.8 ± 1.017988	22.5 ± 1.053565	31.6 ± 0.796576	36.4 ± 0.29023
E. coli	15.5 ± 1.017988	24.8 ± 1.053565	37.4 ± 0.796576	42.1 ± 0.29023
B. subtilis	14.7 ± 0.830682	22.3 ± 0.522047	27.5 ± 0.945163	33.8 ± 0.550757

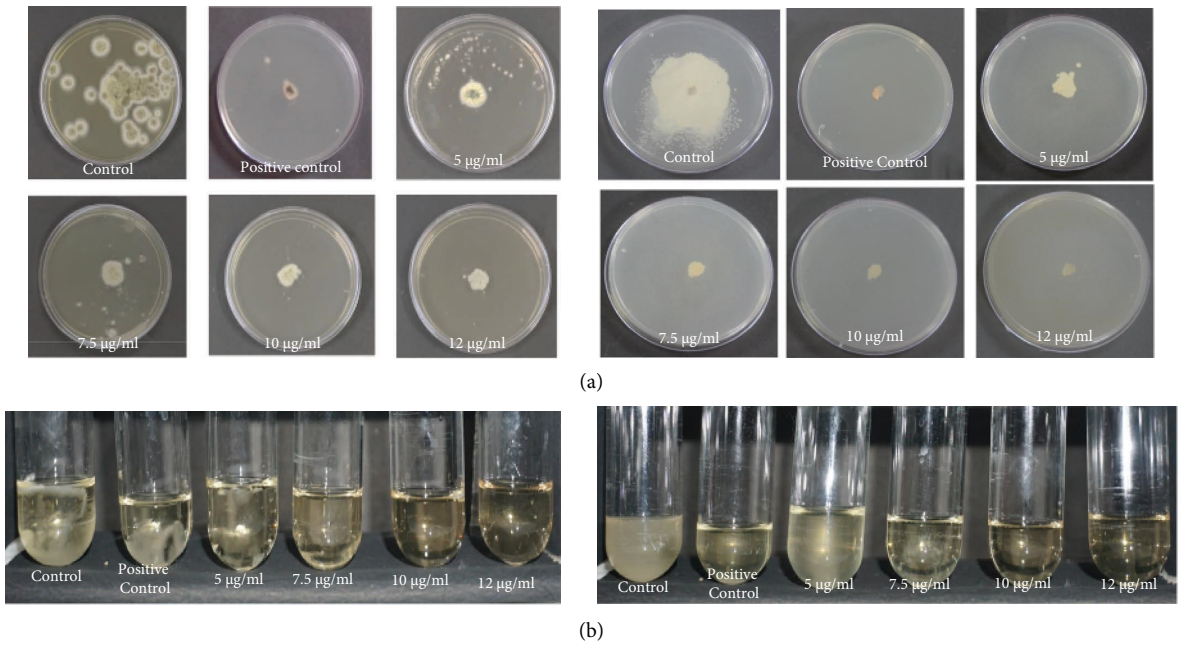

Figure 9: (a) Colony growth assay for *A. niger* and *C. albicans*. (b) Broth dilution assays for *A. niger* and *C. albicans*.

followed by cell-barrier penetration and the release of intracellular metallic silver ions. AgNPs exert this activity via a Trojan-horse mechanism since their initial binding to the cell surface results in permeability alteration and respiration impairment, followed by cell-barrier penetration and alteration and respiration impairment, followed by cell-barrier penetration and intracellular metallic silver ion release [30]. However, various mechanisms of action have been proposed

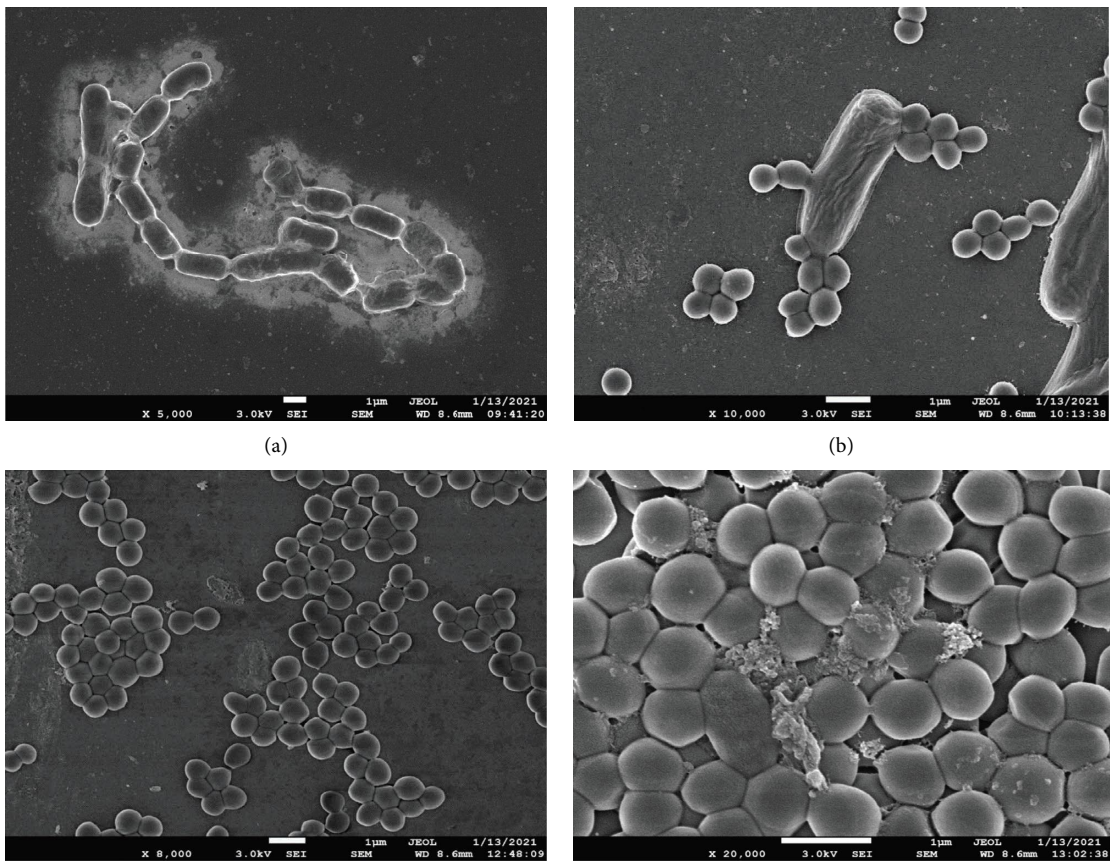

Figure 10: SEM images of (a) B. subtilis culture alone, (b) B. subtilis culture treated with GTAgNPs (c) A. niger culture alone, and (d) A. niger culture treated with GTAgNPs.

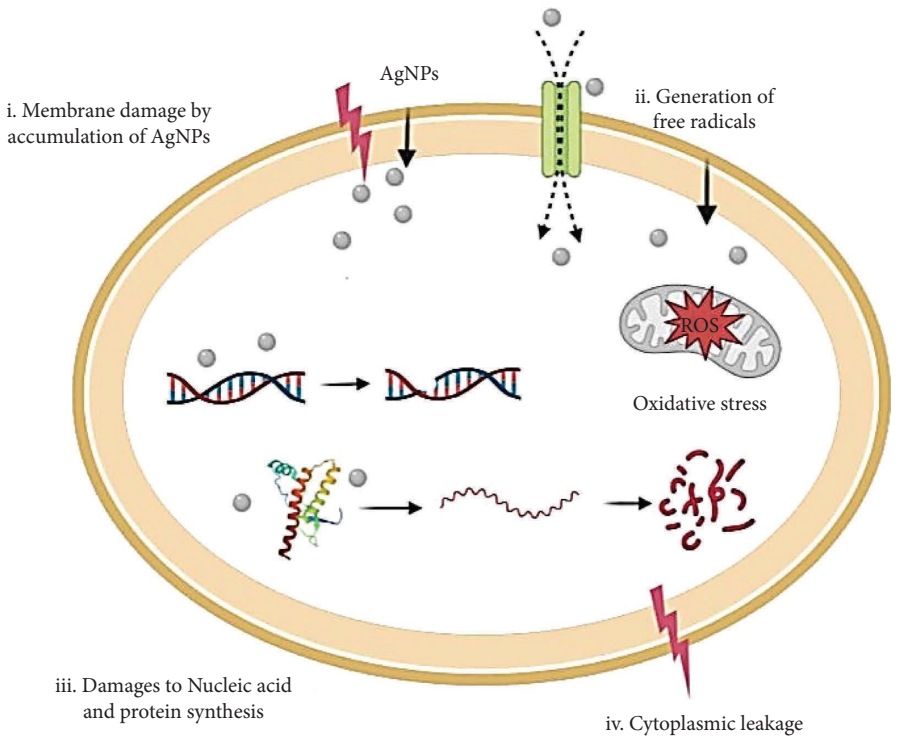

Figure 11: Schematic illustration of antimicrobial mechanism of silver nanoparticles. AgNPs cluster to cause cell membrane damage, making cells porous and causing cytosol leakage. Nanoparticles can generate formation of ROS that have radicalizing effect on microbial cells causing oxidative stress. AgNPs can bind to nucleic acids and can impair the synthesis of the nucleic acid and proteins.

for biogenic AgNPs targeting bacteria and fungi in works published by various groups. Three to four mechanisms of antibacterial and antifungal activity by the biosynthesized AgNPs have been reported in the literature which can be further categorized in different stages as follows: (1) reactive oxygen species (ROS) generation, (2) protein denaturation, (3) binding with cell wall/cell membrane, (4) formation of irregularly shaped pits in the cell membrane that leads to changes in the permeability of the membrane, (5) entry in the cell wall, (6) interruption in the respiratory chain and different pathways, (7) release of lipopolysaccharides and various membrane proteins, and (8) ultimately cell death [2, 34, 35]. The possible mechanism of action has been illustrated in Figure 11.

Therefore, it can be deciphered that nanoparticles help in making the cell membrane unstable, leading to the formation of pores through which AgNPs might get accessibility to the cell and thus impart their inhibitory impact on the microorganism. Though the exact mechanism of antimicrobial activity is not yet deciphered, the mortality of microbes might be due to any of the suggested mechanisms of action of AgNPs on the cell [31, 36, 37].

4. Conclusion

The green approach for the synthesis of AgNPs is associated with an arena of applications in the fields of biomedical, pharmaceutical, and even agricultural activities. The strategy is cost-effective and eco-friendly in the synergism of beneficial aspects of plants with silver. In this study, we have explored the potential of a locally grown berry, *Grewia tenax*, known for its medicinal properties, especially against stomach ailments with the antimicrobial activities of silver. The synthesized AgNPs from the leaf extract of the *Grewia* plant were of 109 nm in size as observed in DLS analysis, and it was at par with the optimized conditions of the BBD tool. The biosynthesized AgNPs showed remarkable antimicrobial activity against bacterial strains such as *B. subtilis*, *E. coli*, *P. aeruginosa*, and *S. aureus* and also against fungi *A. niger* and *C. albicans* along with potent bacterial biofilm inhibition activity. These particles were very active as they brought morphological changes in the cell structure of Gram-positive bacteria and *Aspergillus niger* and *Candida albicans*. These GTAgNPs have high antibacterial efficiency with antibiofilm proficiency and showed high antifungal efficacy which could render them a protective tool in the field of biomedicine specifically with catheters and other medical instruments that might be responsible for infections after medical interventions. The synthesized AgNPs can definitely be used for many bioapplications, but further investigations are required for their safe applications which then can be more useful for the environment and human well-being.

Data Availability

Data sharing is not applicable to this article as no datasets were analysed during the current study. Moreover, all data generated during this study are included in this published article.

Conflicts of Interest

The authors declare that they have no conflicts of interest.

Authors' Contributions

PY was responsible for data curation, formal analysis, methodology, and original writing. MS was responsible for formal analysis, methodology, and manuscript editing. SC was responsible for supervision, resources, project administration, and validation. SN was responsible for supervision, data validation, and resources. NG was responsible for conceptualization, analysis, validation, visualization, and manuscript editing. SC and NG contributed equally to this study.

Acknowledgments

NG acknowledges the financial assistance received in the form of core research grant to the IIS (deemed to be university) from the Department of Science and Technology (DST), Government of India (grant no DST/CURIE-02/2023/IISU (G)).

References

[1] A. Singh, P. K. Gautam, A. Verma et al., "Green synthesis of metallic nanoparticles as effective alternatives to treat antibiotics resistant bacterial infections: a review," *Biotechnology Reports*, vol. 25, Article ID e00427, 2020.

[2] L. Wang, C. Hu, and L. Shao, "The antimicrobial activity of nanoparticles: present situation and prospects for the future," *International Journal of Nanomedicine*, vol. 12, pp. 1227–1249, 2017.

[3] C. M. Crisan, T. Mocan, M. Manolea, L. I. Lasca, F. A. Tăbăran, and L. Mocan, "Review on silver nanoparticles as a novel class of antibacterial solutions," *Applied Sciences*, vol. 11, no. 3, p. 1120, 2021.

[4] A. J. Huh and Y. J. Kwon, "Nanoantibiotics: a new paradigm for treating infectious diseases using nanomaterials in the antibiotics resistant era," *Journal of Controlled Release*, vol. 156, no. 2, pp. 128–145, 2011.

[5] H. Li, X. Zhou, Y. Huang, B. Liao, L. Cheng, and B. Ren, "Reactive oxygen species in pathogen clearance: the killing mechanisms, the adaption response, and the side effects," *Frontiers in Microbiology*, vol. 11, Article ID 622534, 2020.

[6] A. Gupta, S. Mumtaz, C. H. Li, I. Hussain, and V. M. Rotello, "Combatting antibiotic-resistant bacteria using nanomaterials," *Chemical Society Reviews*, vol. 48, no. 2, pp. 415–427, 2019.

[7] N. T. K. Thanh and L. A. W. Green, "Functionalisation of nanoparticles for biomedical applications," *Nano Today*, vol. 5, no. 3, pp. 213–230, 2010.

[8] M. Valodkar, S. Modi, A. Pal, and S. Thakore, "Synthesis and anti-bacterial activity of Cu, Ag and Cu–Ag alloy nanoparticles: a green approach," *Materials Research Bulletin*, vol. 46, no. 3, pp. 384–389, 2011.

[9] S. N. Nangare and P. O. Patil, "Green synthesis of silver nanoparticles: an eco-friendly approach," *Nano Biomedicine and Engineering*, vol. 12, no. 4, pp. 281–296, 2020.

[10] S. Ahmed, M. Ahmad, B. L. Swami, and S. Ikram, "Green synthesis of silver nanoparticles using Azadirachta indica aqueous leaf extract," *Journal of Radiation Research and Applied Sciences*, vol. 9, no. 1, pp. 1–7, 2016.

[11] H. Duan, D. Wang, and Y. Li, "Green chemistry for nanoparticle synthesis," *Chemical Society Reviews*, vol. 44, no. 16, pp. 5778–5792, 2015.

[12] V. Sivamaran, V. Balasubramanian, M. Gopalakrishnan, V. Viswabaskaran, A. Gourav Rao, and S. Selvamani, "Carbon nanotubes, nanorings, and nanospheres: synthesis and fabrication via chemical vapor deposition—a review," *Nanomaterials and Nanotechnology*, vol. 12, Article ID 184798042210794, 2022.

[13] O. Tau, N. Lovergine, and P. Prete, "Adsorption and decomposition steps on Cu(111) of liquid aromatic hydrocarbon precursors for low-temperature CVD of graphene: a DFT study," *Carbon*, vol. 206, pp. 142–149, 2023.

[14] A. Lorusso, V. Nassisi, G. Congedo, N. Lovergine, L. Velardi, and P. Prete, "Pulsed plasma ion source to create Si nanocrystals in SiO2 substrates," *Applied Surface Science*, vol. 255, no. 10, pp. 5401–5404, 2009.

[15] E. Piscopiello, L. Tapfer, M. V. Antisari, P. Paiano, P. Prete, and N. Lovergine, "Formation of epitaxial gold nanoislands on (100) silicon," *Physical Review B: Condensed Matter*, vol. 78, no. 3, Article ID 035305, 2008.

[16] J. Spadavecchia, P. Prete, N. Lovergine, L. Tapfer, and R. Rella, "Au nanoparticles prepared by physical method on Si and sapphire substrates for biosensor applications," *The Journal of Physical Chemistry B*, vol. 109, no. 37, pp. 17347–17349, 2005.

[17] J. Pulit-Prociak and M. Banach, "Silver nanoparticles – a material of the future," *Open Chemistry*, vol. 14, no. 1, pp. 76–91, 2016.

[18] M. S. Akhtar, J. Panwar, and Y. S. Yun, "Biogenic synthesis of metallic nanoparticles by plant extracts," *ACS Sustainable Chemistry and Engineering*, vol. 1, no. 6, pp. 591–602, 2013.

[19] P. Rama, A. Baldelli, A. Vignesh et al., "Antimicrobial, antioxidant, and angiogenic bioactive silver nanoparticles produced using Murraya paniculata (L.) jack leaves," *Nanomaterials and Nanotechnology*, vol. 12, Article ID 184798042110561, 2022.

[20] C. Kamaraj, S. Karthi, A. D. Reegan et al., "Green synthesis of gold nanoparticles using Gracilaria crassa leaf extract and their ecotoxicological potential: issues to be considered," *Environmental Research*, vol. 213, Article ID 113711, 2022.

[21] N. Kulkarni and U. Muddapur, "Biosynthesis of metal nanoparticles: a review," *Journal of Nanotechnology*, vol. 2014, Article ID 510246, 8 pages, 2014.

[22] H. S. A. Al-Shmgani, W. H. Mohammed, G. M. Sulaiman, and A. H. Saadoon, "Biosynthesis of silver nanoparticles from Catharanthus roseus leaf extract and assessing their antioxidant, antimicrobial, and wound-healing activities," *Artificial Cells, Nanomedicine, and Biotechnology*, vol. 45, no. 6, pp. 1234–1240, 2017.

[23] D. Mandal, S. Kumar Dash, B. Das et al., "Bio-fabricated silver nanoparticles preferentially targets Gram positive depending on cell surface charge," *Biomedicine and Pharmacotherapy*, vol. 83, pp. 548–558, 2016.

[24] R. Brause, H. Möltgen, and K. Kleinermanns, "Characterization of laser-ablated and chemically reduced silver colloids in aqueous solution by UV/VIS spectroscopy and STM/SEM microscopy," *Applied Physics B: Lasers and Optics*, vol. 75, no. 6-7, pp. 711–716, 2002.

[25] M. E. Taghavizadeh Yazdi, J. Khara, H. R. Sadeghnia, S. Esmaeilzadeh Bahabadi, and M. Darroudi, "Biosynthesis, characterization, and antibacterial activity of silver nanoparticles using Rheum turkestanicum shoots extract," *Research on Chemical Intermediates*, vol. 44, no. 2, pp. 1325–1334, 2018.

[26] B. Das, A. De, M. Das, S. Das, and A. Samanta, "A new exploration of Dregea volubilis flowers: focusing on antioxidant and antidiabetic properties," *South African Journal of Botany*, vol. 109, pp. 16–24, 2017.

[27] V. Leriche, P. Sibille, and B. Carpentier, "Use of an enzyme-linked lectinsorbent assay to monitor the shift in polysaccharide composition in bacterial biofilms," *Applied and Environmental Microbiology*, vol. 66, no. 5, pp. 1851–1856, 2000.

[28] R. M. Donlan, "Biofilms and device-associated infections," *Emerging Infectious Diseases*, vol. 7, no. 2, pp. 277–281, 2001.

[29] G. Arya, R. Mankamna Kumari, N. Sharma et al., "Evaluation of antibiofilm and catalytic activity of biogenic silver nanoparticles synthesized from *Acacia nilotica* leaf extract," *Advances in Natural Sciences: Nanoscience and Nanotechnology*, vol. 9, no. 4, Article ID 045003, 2018.

[30] G. Arya, R. M. Kumari, N. Sharma et al., "Catalytic, antibacterial and antibiofilm efficacy of biosynthesised silver nanoparticles using Prosopis juliflora leaf extract along with their wound healing potential," *Journal of Photochemistry and Photobiology B: Biology*, vol. 190, pp. 50–58, 2019.

[31] M. Singhal, S. Chatterjee, A. Kumar et al., "Exploring the antibacterial and antibiofilm efficacy of silver nanoparticles biosynthesized using punica granatum leaves," *Molecules*, vol. 26, no. 19, p. 5762, 2021.

[32] M. A. Pfaller and D. J. Diekema, "Epidemiology of invasive candidiasis: a persistent public health problem," *Clinical Microbiology Reviews*, vol. 20, no. 1, pp. 133–163, 2007.

[33] S. Bowman, S. J. Free, and S. J. Free, "The structure and synthesis of the fungal cell wall," *BioEssays: News and Reviews in Molecular, Cellular and Developmental Biology*, vol. 28, pp. 799–808, 2006.

[34] H. Chandra, P. Kumari, E. Bontempi, and S. Yadav, "Medicinal plants: treasure trove for green synthesis of metallic nanoparticles and their biomedical applications," *Biocatalysis and Agricultural Biotechnology*, vol. 24, Article ID 101518, 2020.

[35] S. Rajeshkumar and L. V. Bharath, "Mechanism of plant-mediated synthesis of silver nanoparticles-a review on biomolecules involved, characterisation and antibacterial activity," *Chemico-Biological Interactions*, vol. 273, pp. 219–227, 2017.

[36] I. X. Yin, J. Zhang, I. S. Zhao, M. L. Mei, Q. Li, and C. H. Chu, "The antibacterial mechanism of silver nanoparticles and its application in dentistry," *International Journal of Nanomedicine*, vol. 15, pp. 2555–2562, 2020.

[37] E. O. Mikhailova, "Silver nanoparticles: mechanism of action and probable bio-application," *Journal of Functional Biomaterials*, vol. 11, no. 4, p. 84, 2020.